Performance evaluation of a direct-conversion flat-panel detector system in imaging and quality assurance for a high-dose-rate ^{192}Ir source

Yoshinori Miyahara,[1] **Hajime Kitagaki,**[2] **Taisuke Inomata**[3]

[1] Department of Radiology, Shimane University Hospital, 89-1 Enya, Izumo, Shimane, Japan

[2] Department of Radiology, Shimane University Faculty of Medicine, 89-1 Enya, Izumo, Shimane, Japan

[3] Department of Radiation Oncology, Shimane University Faculty of Medicine, 89-1 Enya, Izumo, Shimane, Japan

E-mail: miyahara@med.shimane-u.ac.jp

Abstract

In high-dose-rate (HDR) brachytherapy, a direct-conversion flat-panel detector (d-FPD) clearly depicts a ^{192}Ir source without image halation, even under the emission of high-energy gamma-rays. However, it was unknown why iridium is visible by the d-FPD. The purpose of this study was to clarify why the source is visible using by physical imaging characteristics. In addition, we verified the accuracy of the source positions within the clinical applicator. The physical imaging characteristics of d-FPD were evaluated on depicting a source, which emits gamma-rays, regarding the modulation transfer functions (MTF), noise power spectral (NPS), contrast transfer functions (CTF), and linearity of d-FPD to high-energy gamma-rays. The acquired data included X-rays: [X], gamma-rays: [γ], dual-rays (X+γ): [*D*], and subtracted data for depicting the source ([*D*] - [γ]). In the quality assurance (QA) test for the positional accuracy of a source core, the coordinates of each dwelling point were compared between planned and actual source core positions using both CT/MR and Fletcher applicators. The profile curves of [X] and ([*D*] - [γ]) matched well on MTF and NPS. Contrast resolutions of [*D*] and [X] were equivalent. A strong positive linear correlation was found between the output data of [γ] and source strength (r2 > 0.99). With regard to the accuracy of the source core position, the largest coordinate difference (3D-distance) was noted at the maximum curvature of the CT/MR and Fletcher applicators showing 1.74 ± 0.02 mm and 1.01 ± 0.01 mm, respectively. A d-FPD system provides high-quality images of a source, even

when high-energy gamma-rays are emitted to the detector. And positional accuracy tests with clinical applicators are useful in identifying source positions (source movements) within the applicator.

Key words: high-dose-rate brachytherapy, ^{192}Ir source, quality assurance direct-conversion flat-panel detector, physical imaging characteristics,

1. INTRODUCTION

A high-dose-rate (HDR) ^{192}Ir source emits gamma photons (mean energy of 0.38 MeV), beta-rays and characteristic x-rays from a radioactive solid core, which is enclosed in a stainless steel capsule and attached to a stainless steel cable. With conventional devices such as image intensifier, it was not possible to clearly a source image due to image halation. However, the FPD system has made it possible to depict a source without image halation. In particular, after acquiring data with a d-FPD system (Shimadzu Co., Kyoto, Japan), the incident photons are directly converted to the electrical charge through the amorphous selenium photoconductor (Zhao *et al* 2005, Kasap *et al* 2006). Thereby the scattering of light in the detector does not occur in the d-FPD system, providing a high detective quantum efficiency (DQE) and a wide dynamic range for incident photons, enabling the acquisition of a high-quality image. However, the performance evaluation of the d-FPD system has been difficult on depicting a radioactive source due to incident dual-rays simultaneously emitted to the detector (X-rays from the generator and high-energy gamma-rays from the source). There are no articles describing how gamma-rays affect image quality in source imaging. To overcome this problem, we developed a subtraction technique to process raw data obtained from the dual-rays. In addition, we performed a QA of a source positional accuracy test (Kubo *et al* 1998, Wilkinson *et al* 2006, Nath *et al* 1997) using clinical applicators. The difference between the planned source position and the actual source core position was evaluated based on 3-dimensional vectors (Smith *et al* 2016, Smith *et al* 2017). Our purpose was to evaluate the performance of a d-FPD system for the imaging of a source, and to establish a new quality assurance test method to promote source positional accuracy using the d-FPD system.

2. METHODS AND MATERIALS

2.1. Concept and experimental definition

In order to depict a radioactive ^{192}Ir source (microSelectron HDR v2r, Nucletron BV, Veenendaal, The Netherlands) by radiography, dual-rays (high-energy gamma-rays and X-rays from generator) must be incident on the detector. Our d-FPD system is for the diagnostic X-ray system, not for high-energy X-rays and gamma-rays. The possibility of image distortion or blurring due to high-energy gamma-rays can't be denied. What we should evaluate is that the X-ray for depicting a source is not affected by high-energy gamma rays. Generally, the MTF and NPS evaluates from raw data (unprocessed data). In this study, we obtained the X-rays data for depicting a source by the method of subtracting raw data. Figure 1 shows the concept of subtraction methods for depicting a source.

The symbol [D] means dual-rays (X-rays and gamma-rays) that are simultaneously incident on the detector, and [γ] means gamma-rays that were incident on the detector alone. We evaluated whether the dynamic range of diagnostic X-ray system can adapt to high-energy gamma-rays. For the acquisition of [γ], the detector can receive pure gamma-rays during irradiation while exposing the detector to dummy X-rays (40 kVp, 50 mA, 20 msec) emitted from the generator shielded with lead. In this way, X-rays were not incident to the detector. The subtracted data ([D] - [γ]) are pure X-rays effective for depicting a source.

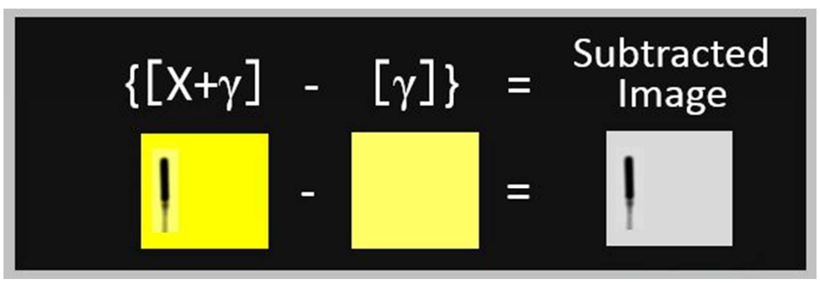

Figure 1. Concept of subtraction methods. The subtracted image means pure X-rays for depicting a source.

2.2. Physical characteristics of d-FPD for high-energy gamma-rays

We had investigated image halation and non-linear strain which caused degradation of raw data and image processing due to the presence of a source. As physical imaging characteristics of d-FPD for depicting a source, MTF and NPS were measured. Generally, MTF was used as the resolution characteristic, and NPS was used as the noise characteristic of the image quality evaluation. In this study, we evaluated whether d-FPD is affected by the presence of the source by using each function, not the evaluation of specific resolution and noise characterization for the d-FPD.

Since high-energy gamma-rays, the MTF and NPS profile curves become non-uniform and rough, hindering the analysis. Therefore, we attempted to obtain the raw data of ([D] - [γ]) by subtracting, in addition, it is relative comparison utilizing "function" called MTF or NPS (Giger and Doi 1984, Fujita *et al* 1992, Cunningham and Reid 1992).

MTF measurement was conducted by the same geometric layout as ordinary acquisition of a source image as Figure 2. We basic premised that the source can be depicted even at the air kerma strength (Sk) of 40.66 mGy$\cdot$ m^2 $\cdot$ h^{-1} after the source exchange. Under that condition, the MTF measurement dose was determined by the automatic dose required for a source imaging. The imaging conditions as follows: 59 kVp, 35 mA, a 5.0 msec pulse width, 43.18 cm FOV, 2 × 2 binning, and at a 110 cm source to image distance (SID) with 1.0 mm thick tungsten edge phantom (Shimadzu Co., Kyoto, Japan). The tungsten edge and anti-scatter grids of the detector were set in the same direction. In order to avoid strong penetration of the tungsten edge itself due to gamma rays, a source was placed at a position not overlapping the tungsten edge. In MTF measurement, ([D] - [γ]) and [X] were compared.

The configuration of NPS measurement is shown in Figure 3. An aluminum plate ($45 \times 45 \times 4.0$ cm^3) was used as an absorber, and a source was placed off-center of the aluminum plate. The images were acquired at 68 kVp, 560 mA, 8.0 msec pulse width, a 43.18 cm FOV, 2×2 binning, 15 frames per second, 110 cm SID, and with an additional filter (1.0 mm Al + 10.0 μm Au). Four NPS profile curves of [X], [γ], [D], and ([D] - [γ]) were obtained. NPS were not normalized. The subtracting analyses were conducted using by Shimadzu software. In order to avoid degradation of the signal-to-noise ratio through subtraction, the images were obtained from multi-frames by integration processing.

In CTF measurement (Nill 2001) for obtaining contrast transfer functions from chart images, we evaluated the influence of high-energy gamma-rays on image quality. A resolution test-patterns (copper chart) of a Japanese Society of Gastrointestinal Imaging (JSGI) phantom (Toreck Co. Yokohama, Japan) as shown in Figure 4(a) were used along with an added copper plate ($115 \times 115 \times 2.0$ mm^3) at three different FOV (15.24, 30.48, and 43.18 cm) for images of [D] and [X]. CTF was defined as the ratio between the reference and object frequencies, which was calculated by the maximum (black line) and minimum (white line) values of each region of interest (ROI) in the test-pattern. CTFs were calculated by the maximum (black lines: B1, C1, and D1) and minimum (white lines: B2, C2, and D2) values in each ROI of the test-pattern image as Figure 4(b). Each CTF was calculated as following equation (1):

$$\mathrm{CTF}(u) = \mathrm{Object\ (max\text{-}min)} / \mathrm{Reference\ (max\text{-}min)} = \mathrm{B1\text{-}B2} / \mathrm{A1\text{-}A2} \quad \cdots \quad (1)$$

The radioactivity of ^{192}Ir decays with a half-life of 74 days; thus, the source is to be exchanged every three months. The source strength (Sk) when measuring MTF, NPS and CTF was 40.66 mGy・m^2・h^{-1}.

Linearity measurement of d-FPD for high-energy gamma-rays was conducted weekly. For the acquisition of images solely by gamma-rays, dummy X-rays were emitted while shielding the X-ray generator with lead (Figure 5). The Acquisition conditions for each measurement was 40 kVp, 50 mA, 20 msec. A source was placed at the rotation center (isocenter) by isocenter display of the C-arm systems, and the output value (digital value / pixel) of the d-FPD was measured by setting a square ROI in the gamma-ray image. In order to evaluate reproducibility and mechanical variations in image acquisition, a gamma-rays image was acquired five times by consecutively setting and removing the devices. Considering the decay of the source, measurements were conducted within 30 minutes. That is to say, the time required for one measurement is approximately 5 minutes.

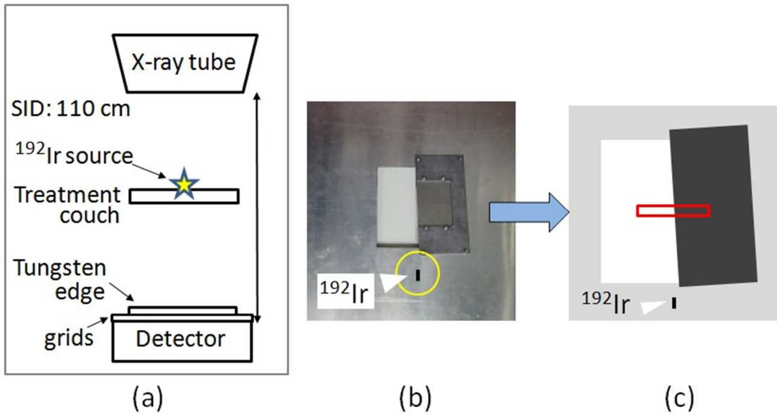

Figure 2. Illustration of the MTF measurement (a), arrangement of tungsten edge and illustrated a source (yellow circle) (b). A source was placed in a position not overlapping with the tungsten edge, and the profile curve was obtained from a region in the rectangular red-box (c).

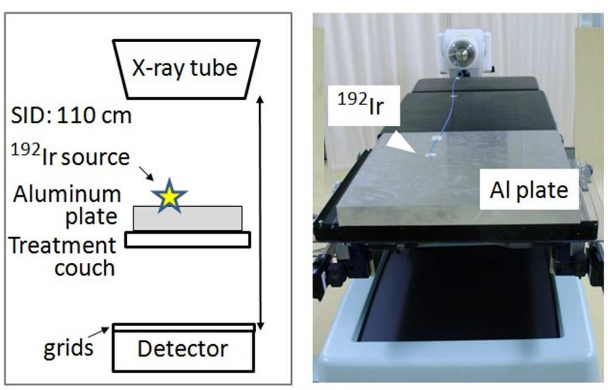

Figure 3. Illustration of the NPS measurement (left) and layout of a source with an aluminum plate (right).

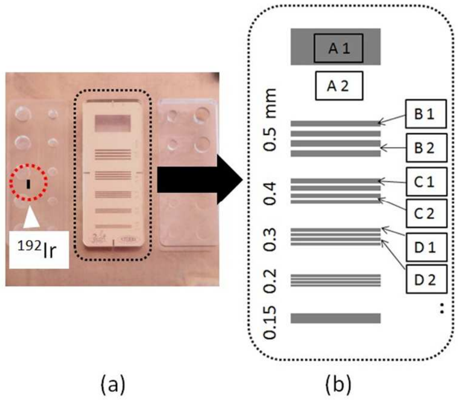

Figure 4. Resolution test-patterns in the JSGI phantom. A source (illustrated) was placed at a position (red circle) not overlapping with the test-pattern chart (a), and illustration of the test-patterns (b).

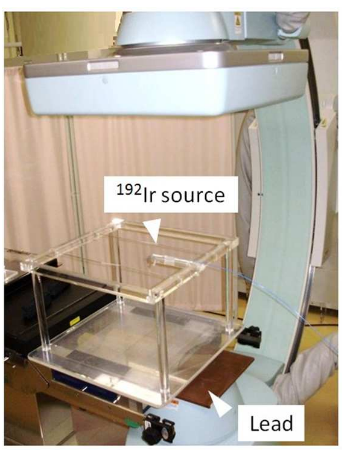

Figure 5. Configuration of the weekly linearity measurement of [γ]. A source was placed at rotation center (isocenter) of the C-arm on an acrylic box. For acquisition of the image solely by gamma-rays, dummy X-rays were emitted while shielding the X-ray generator with a lead plate.

2.3. Quality assurance of the source dwell positions

The source positional accuracy test was conducted using reconstruction jig and two different types of clinical applicators: CT/MR-compatible ovoid and Fletcher-Williamson (F-W) tandem (Figure 6). The reconstitution jig consists of a base plate and a C-shaped attachable structure. The radio-opaque fiducial markers (approximately 2.0 mm) are embedded the base plate and the reconstitution jig (front plane and both side). The three-dimensional (3-D) coordinates were constructed by semi-orthogonal method from the d-FPD images (frontal and lateral views) obtained both reconstruction jig and an applicator with radio-opaque catheter (markers). The semi-orthogonal method is a well-established in 3-D construction in brachytherapy. A size of each catheter marker is approximately 1.0 mm, and the planning of the source dwell positions were conducted by the method of the describing points. A spherical metal marker (diameter of 2.0 mm) in a cubical phantom (Varian Medical Systems, CA, USA) was defined as the center of the Applicator Coordinate System (ACS). The planned measurement points and movement steps of the CT/MR and F-W applicators were 14 points at 5.0 mm, and 15 points at 2.5 mm, respectively. After the plot planning, the source core images with each applicator were acquired using d-FPD from two directions. Each image was conducted with one-shot radiography of each dwell position (e.g. 28 images were obtained by each of the frontal and lateral view in case of 14 dwell points). The imaging conditions of a source core in the CT/MR and F-W applicators were 60 kVp, 250 mA, 28 msec and 67 kVp, 250 mA, 28 msec respectively. The differences in source coordinates between the planned and actual source core positions were measured three times for a plan.

The applicator setup, source positional planning and data analysis were using the brachytherapy treatment planning system (Oncentra® Brachy v.4.3, Elekta AB, Stockholm, Sweden).

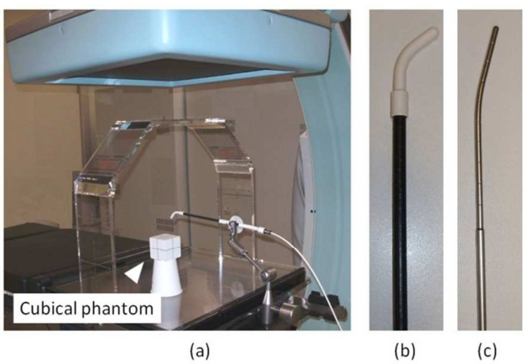

Figure 6. Photographs of the source positional accuracy test setting with the d-FPD (a), a CT/MR-compatible ovoid applicator (45 degrees) (b), and a Fletcher-Williamson tandem applicator (15 degrees) (c).

3. RESULTS

3.1. Physical characteristics

We obtained ([*D*] - [γ]) curves of both MTF (Figure. 7 (a) and NPS (Figure 7 (b). The Nyquist frequency was 1.67 lp/mm in the image obtained by 2 × 2 binning (pixel pitch: 300 μm). A small peak (around 1.6 lp / mm) observed on each of the MTF and NPS curves was due to the presence of anti-scatter grids. In MTF and NPS, the two profile curves of [X] and ([*D*] - [γ]) matched very well. Additionally, on NPS measurement, four kinds of data, [X], [γ], [*D*], and ([*D*] - [γ]), could be acquired. However, such a small peak associated with the anti-scatter grids did not appear in the profile curves of [γ] alone.

CTF was measured using test-pattern images obtained by three different FOV settings. In each FOV, two profile curves of [X] and [*D*] almost matched or [*D*] was slightly higher (Figure 8). The image quality of d-FPD was not affected by the high-energy gamma-rays.

Figure 9 shows the correlation between the source strength (Sk) and output value (digital value / pixel) of d-FPD. The dynamic range of d-FPD for high-energy gamma-rays was wide, showing excellent linearity (R2 = 0.99, p $<$ 0.001).

In the analysis with five gamma-ray images acquired by setting and removing the devices consecutively, 1σ of the output value of d-FPD was 1.67, and the derived standard uncertainty (type-A) was 1.57.

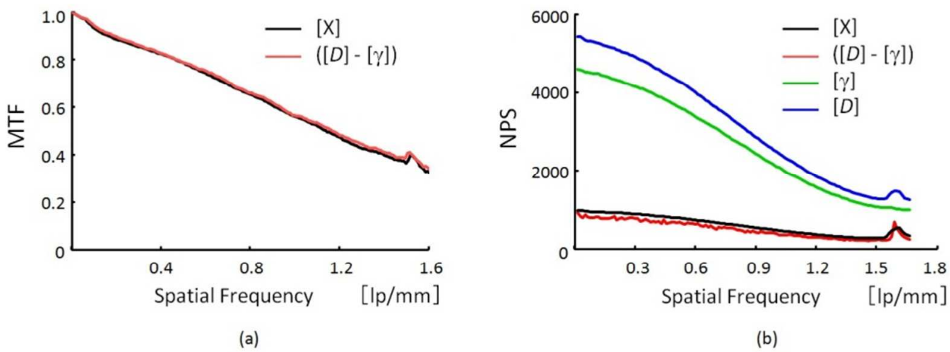

Figure 7. Results of MTF (a) and NPS (b).

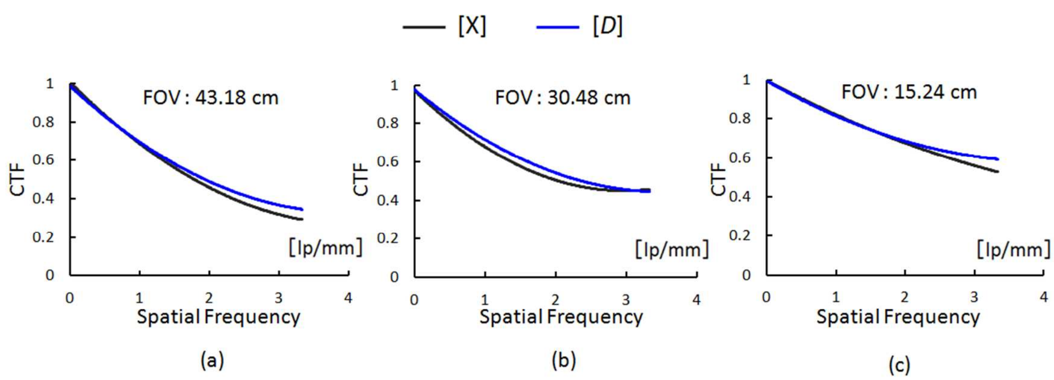

Figure 8. Results of CTF for three different FOV settings. Exposure conditions were: (a) 77 kVp, 288 mA, 40 msec, (b) 78 kVp, 291 mA, 40 msec, and (c) 78 kVp, 291 mA, 40 msec.

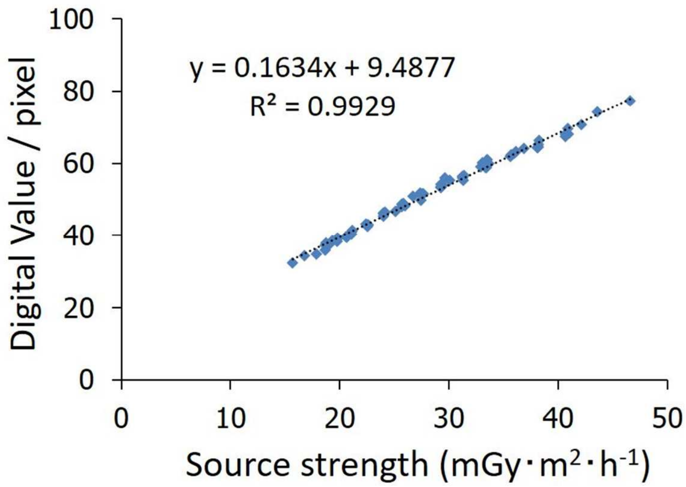

Figure 9. Correlation between the source strength and output value of d-FPD.

3.2. Quality assurance of the source positions

The source cores with two different types of applicators were clearly depicted, and the coordinates of the source core could be identified. Table 1 shows the summary of source coordinates differences of each axis for the two types applicators. The 1σ (mean) of the displacement at all dwell points for the F-W applicator and CT/MR applicator were 0.04 mm (largest: 0.08 mm) and 0.05 mm (largest: 0.17 mm) respectively.

Figure 10 shows the results of the source positional accuracy test using F-W tandem 15° (Figure 10 a) and CT/MR ovoid 45° (Figure 10 b). The line graph shows the mean values and standard deviation (SD) of the planned and the actual source core positions. Three measurements were conducted for a plan. In the X (right-left) and Y (superoinferior) axes of the both applicators, coordinate differences of less than 1.0 mm were observed. On the other hand, the maximum coordinate differences of 0.8 mm (F-W tandem) and 1.7 mm (CT/MR ovoid) were observed on the Z (anteroposterior) axis at the curved portion of the applicators. Also in the 3D distance, the CT/MR ovoid applicator had a larger coordinate difference at the curved portion. However, the maximum 3-D distance was less than 2.0 mm with both applicators.

Each uncertainty in the source positional accuracy test was estimated as follows: 1) 0.1 mm from the standard deviation by three measurements, 2) 0.3 mm from the size of the marker, 3) 0.3 mm from the size of the source core, 4) 0.1 mm from the size of the pixel (0.15 mm). Based on these uncertainties, expanded measurement uncertainty (k = 2) of 0.8 mm was estimated.

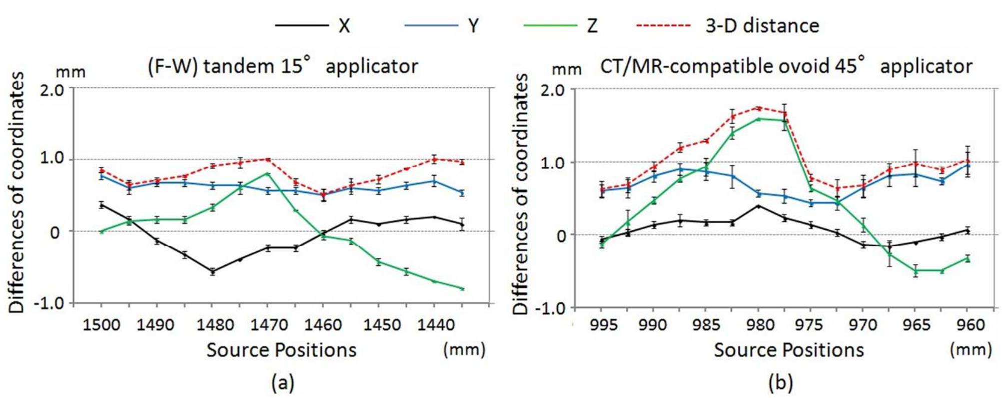

Figure 10. Source positional accuracy test using an F-W applicator (a), and a CT/MR applicator (b). The measurements were performed three times for a

plan in three coordinate axes (X: Right-Left, Y: Superoinferior, Z: Anteroposterior). The line graphs shows the mean (±1σ) at each dwell position.

Table 1. Summary of source coordinates differences of each axis. (mm)

Applicator	N	Axis	Max	Min	Mean	1σ (mean)	1σ (max)
(F-W) tandem	42	ΔX	0.4	0.0	0.23	0.04	0.08
		ΔY	0.8	0.4	0.62	0.05	0.08
		ΔZ	0.8	0.0	0.37	0.04	0.08
CT/MR ovoid	45	ΔX	0.4	0.0	0.14	0.05	0.09
		ΔY	1.2	0.3	0.62	0.06	0.09
		ΔZ	1.7	0.0	0.66	0.08	0.17

4. DISCUSSION

Physical image properties of multi-rays are difficult to evaluate. In the geometrical arrangement in these C-arm types of FPD system, the strength of incident gamma-rays are not attenuate for measurement of MTF, even if the distance between the source and detector is increased. That is, the high-energy gamma-rays passes through the tungsten edge. In this study, MTF and NPS were evaluated by subtraction procedures for all raw data. The subtracted data ([*D*] - [γ]) indicate pure X-rays for depicting a source. The data of ([*D*] - [γ]) and [X] matched well for the MTF and NPS results; therefore, the X-rays for depicting a source are considered unaffected by high-energy gamma-rays.

In our investigation, we paid attention to the small peaks derived by the anti-scatter grids in the curves of Figure 7. However, in NPS measurement, such a small peak was not shown in the curve of [γ], possibly due to strong gamma-rays from the source which passed through the anti-scatter grids. However, in [X], [*D*], and ([*D*] - [γ]) curves, a peak appeared because they contained X-rays data including the effect of anti-scatter grids. This means that d-FPD would identify and differentiate X-rays from gamma-rays as electrical charges, even when these are simultaneously transmitted to the detector. In other words, the data subtraction procedures are considered innovative and potentially a breakthrough technique for the analysis of each spatial frequency characteristic in multi-rays.

In CTF measurement, the image sharpness is an important factor. The higher the input-dose to d-FPD, the greater the improvement of image sharpness. The input-dose of [*D*] was several percent higher than [X]. As shown in Figure 8, the profile curves of [X] and [*D*] almost matched or [*D*] was slightly higher in each FOV. Thus, the image quality of d-FPD is considered unaffected by high-energy gamma-rays.

For the linearity test of d-FPD to high-energy gamma-rays, we collected data weekly for a year. FPD is constantly detecting the incident photons while high-voltage power supply is applied. By pressing the X-ray trigger button, the FPD receives the exposure signal and the incident photons are readout. In this measurement, X-rays are not incident to a d-FPD due to the shielding of the generator, but a trigger button must pushed. Therefore, the possibility of mechanical noise cannot be ruled out. If the acquisition time changes, the output (digital value/pixel) may change. But these gamma-ray images were processed images. Since the acquisition time is constant every week, the correlation does not change. From these measurements, it was found that the d-FPD has a wide dynamic range for high-energy gamma-rays, as well as excellent linearity between output values of d-FPD and the source strength.

The positional accuracy test of a source core is one of the important aspects of quality assurance, because the core of the ^{192}Ir emits gamma-rays. A radioactive solid core of the model mHDR-v2r has a length of 3.5 mm, and a stainless steel capsule is fixed at the distal end of a stainless steel cable. Additionally, there is no core in the dummy source. Regarding the source positional accuracy test using the d-FPD image, it has reported (Miyahara *et al* 2015) that the source positional precision has controlled within ± 1.0 mm in the check ruler. Many other methods of source positional accuracy using imaging panel (Fonseca *et al* 2015) and EPID (Smith *et al* 2013) have also reported. In this study, we conducted the source positional verification using the clinical applicators in accordance with the clinical treatment.

In the treatment planning, the source core positions were predetermined as points on the image of a radio-opaque catheter. In either axis, slight mismatches of coordinates occur by distortion of the radio-opaque catheter and the looseness of the source itself. In the CT/MR ovoid applicator, a coordinate difference of 1.7 mm was observed at the curved portion between the planned position and the source core position. This is because the actual ^{192}Ir capsule-tip moves along the inner-diameter with the certain angle (Figure 11). Although the effect of the dose distribution was not verified in this our study, it is necessary to pay attention to the possibility that the dose distribution may be different at the curved portions of large curvature applicators. The recommendation of the American Association of Physicists in Medicine (AAPM) for source position accuracy is ± 2.0 mm relative to the applicator system (Nath *et al* 1997). In this study, all positional errors were within the acceptable range.

The uncertainty in the applicator coordinate system is whether points can be set at the center of all markers. This depends on visual recognition as well as pixel and marker size. We consider that uncertainty may be reduced by adjusting the image (magnification, brightness and contrast) to the optimum condition on the monitor. As shown in Table 1, since the standard deviations of the source dwell positions on each axis was almost within 0.1 mm (0.17 mm at the maximum), it was found that the high-reproducibility of the measurement and the high-precision of the source dwell positions. The 1σ of the measurements on each axis were slightly larger in CT/MR applicator. Additionally, a standard deviation of 0.17 mm was observed at the uncurved portion of the CT/MR applicator. This is due to the difference in the sizes of the inner-diameter (F-W tandem: approximately 1.5 mm, CT/MR ovoid: 3.0 mm). Depending on the sizes of the inner-diameter, the standard deviation may increase. These factors are increase the uncertainty.

In remote afterloading brachytherapy, the coincidence of the pre-loaded source positions and the actual source positions is important. Many methods have been reported for the source positional accuracy test (Jangda *et al* 2011, Awunor *et al* 2013, Humer *et al* 2015, Fonseca *et al* 2017). Even in recent years, irradiation accidents (Valentin 2005) have occurred in some facilities, due to positional mismatches between the planned position and the actual source position. Therefore, the importance of the source positional accuracy test has increased. Okamoto et al (2017) has developed the phantom and evaluated the source position using both clinical applicators and radiochromic film. They also investigated the source positional uncertainty from 12 facilities in Japan.

In our study, we conducted the source positional accuracy test from the source core images in clinical applicators using by the d-FPD system. Since the high-energy gamma-rays are not affect the image quality, source core images in carbon and metallic applicators could be acquired without image halation. The quality assurance of source position by clear images may reduce measurement uncertainty. Our method to evaluate the mismatches source positions between pre-loaded and after-loaded in a clinical applicator is clinically relevant.

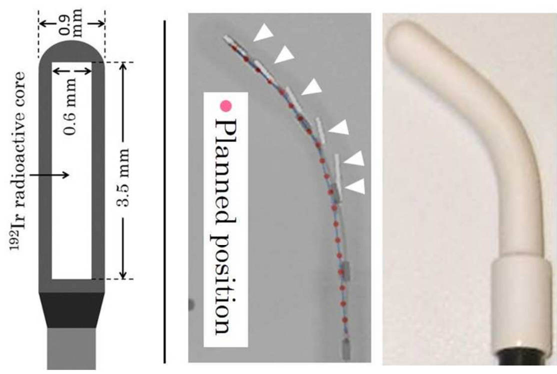

Figure 11. Schematic drawing of a MicroSelectron mHDR-v2r brachytherapy source (left). A fusion image of ^{192}Ir core (arrow) movements and a CT/MR-compatible ovoid applicator with a radio-opaque catheter (right).

5. CONCLUSIONS

With d-FPD, X-rays for depiction of a ^{192}Ir source are unaffected by high-energy gamma-rays, even though these are simultaneously transmitted with X-rays to the detector. This is because the d-FPD converts incident photons directly into electrical charges through amorphous selenium photoconductors, and has a wide dynamic range and excellent linearity to the high-energy gamma-rays. Therefore, d-FPD is considered capable of providing high-quality images of a ^{192}Ir source core without image halation.

An awareness of the operational conditions of the ^{192}Ir source is necessary, as several factors are involved in the source positional errors. The ^{192}Ir source positions are clearly visible during intracavitary brachytherapy using d-FPD. Therefore, the source positional accuracy test with clinical applicators is useful for quality assurance of d-FPD, as well as contributing to the accuracy of HDR brachytherapy.

ACKNOWLEDGEMENTS

The authors are grateful for assistance of radiological technologists at the Department of Radiology of Shimane University Hospital.

CONFLICTS OF INTEREST

The authors declare no conflict of interest.

REFERENCES

Awunor O.A, Dixon B and Walker C 2013 Direct reconstruction and associated uncertainties of 192Ir source dwell positions in ring applicators using gafchromic film in the treatment planning of HDR brachytherapy cervix patients *Phys. Med. Biol.* 58 3207-25

Cunningham I. A and Reid B. K 1992 Signal and noise in modulation transfer function determinations using the slit, wire, and edge techniques. *Med. Phys.* 19 1037-44

Fonseca G P, Bosch M R V D, Voncken R, Podesta M and Verhaegen F 2017 A novel system for commissioning brachytherapy applicators: example of a ring applicator *Phys. Med. Biol.* 21 8360-75

Fonseca G P, Podesta M, Bellezzo M, Bosch M R V D, Lutgens L, Vanneste B G L, Voncken R, Limbergen E J V, Reniers B and Verhaegen F 2017 Online pretreatment verification of high-dose rate brachytherapy using an imaging panel *Phys. Med. Biol.* 62 5440-61

Fujita H, Tsai D.Y, Itoh T, K. Doi, Morishita J, Ueda K and Ohtsuka A 1992 A simple method for determining the modulation transfer function in digital radiography. *IEEE Trans. Med. Imaging.* 11 34-39

Giger M. L and Doi K. 1984 Investigation of basic imaging properties in digital radiography. I . Modulation transfer function. *Med. Phys.* 11 287-95

Humer I, Kirisits C, Berger D, Trnková P, Pötter R and Nesvacil N 2015 Improved source path localisation in ring applicators and the clinical impact for gynecological brachytherapy. *J Contemp Brachytherapy.* 7 239-243

Jangda A. Q, Hussein S and Rehman Z 2011 A new approach to measure dwell position inaccuracy in HDR ring applicator – quantification and corrective QA. *J. Appl. Clin. Med. Phys.* 12 3-13

Kasap S. O, Kabir M. Z and Rowlands J. A 2006 Recent advances in X-ray photoconductors for direct conversion X-ray image detectors *Curr. Appl. Phys.* 6 288-292

Kubo H. D, Glasgow G. P, Pethel T. D, Thomadsen B. R and Williamson J. F 1998 High dose-rate brachytherapy treatment delivery: report of the AAPM Radiation Therapy Committee Task Group No. 59 *Med Phys.* 25 375-403

Nath R, Anderson L. L, Meli J. A, Olch A. J, Stitt J. A and Williamson J. F 1997 Code of practice for brachytherapy physics: Report of the AAPM Radiation Therapy Committee Task Group No. 56. *Med. Phys.* 24 1557-98

Nill N. B 2001 Conversion between sine wave and square wave spatial frequency response of an imaging system. *MITRE Technical Report.* MTR 01B0000021

Smith R L, Taylor M L, McDermott L N, Haworth A, Millar J L and Franich R D 2013 Source position verification and dosimetry in HDR brachytherapy using an EPID *Med. Phys.* 40 111706

Smith R L, Haworth A, Panettieri V, Millar J L and Franich R D 2016 A method for verification of treatment delivery in HDR prostate brachytherapy using a flat panel detector for both imaging and source tracking *Med. Phys.* 5 2435-42

Smith R L, Haworth A, Panettieri V, Millar J L and Franich R D 2017 3D catheter reconstruction in HDR prostate brachytherapy for pre-treatment verification using a flat panel detector *Phys Med.* 39 121-131

Valentin J. 2005 Prevention of high-dose-rate brachytherapy accidents *ICRP Publication 97. Ann ICRP* 35 1–51

Wilkinson DA 2006 High dose rate (HDR) brachytherapy quality assurance: a practical guide *Biomed Imaging Interv J.* 2 1-7

Zhao W, Hunt D. C, Tanioka K and Rowlands J. A 2005 Amorphous selenium flat panel detectors for medical applications *Nucl. Instrum. Methods. Phys. Res. A.* 549 205-209